

The Onset of Thermalisation in Finite-Dimensional Equations of Hydrodynamics: Insights from the Burgers Equation

Divya Venkataraman^{1,*} and Samriddhi Sankar Ray^{1,†}

¹*International Centre for Theoretical Sciences, Tata Institute of Fundamental Research, Bangalore 560089, India*

Solutions to finite-dimensional (all spatial Fourier modes set to zero beyond a finite wavenumber K_G), inviscid equations of hydrodynamics at long times are known to be at variance with those obtained for the original infinite dimensional partial differential equations or their viscous counterparts. Surprisingly, the solutions to such Galerkin-truncated equations develop sharp localised structures, called *tygers* [Ray, et al., Phys. Rev. E **84**, 016301 (2011)], which eventually lead to completely thermalised states associated with an equipartition energy spectrum. We now obtain, by using the analytically tractable Burgers equation, precise estimates, theoretically and via direct numerical simulations, of the time τ_c at which thermalisation is triggered and show that $\tau_c \sim K_G^\xi$, with $\xi = -4/9$. Our results have several implications including for the analyticity strip method to numerically obtain evidence for or against blow-ups of the three-dimensional incompressible Euler equations.

INTRODUCTION

A microscopic understanding of turbulent flows have been amongst the most challenging problems in statistical physics for many years. Central to this challenge is adapting well-developed tools of statistical mechanics for dissipative and out-of-equilibrium turbulent flows. The early efforts in this direction, due to E. Hopf [1] and T. D. Lee [2], treated the ideal (inviscid) equations of hydrodynamics as a finite-dimensional, Galerkin-truncated system and obtained equipartition solutions with an energy spectrum, in three dimensions, $E(k) \sim k^2$, at variance with the Kolmogorov result $E(k) \sim k^{-5/3}$ for dissipative turbulent flows [3].

A major stumbling block in developing a framework to understand out-of-equilibrium turbulent flows in the language of classical equilibrium statistical mechanics is that a microscopic, Hamiltonian formulation of fluid motion with statistically steady states characterised by an invariant Gibbs measure inevitably fails. This is because a self-consistent macroscopic point of view will invariably lead to an irreversible energy loss and thus a dissipative hydrodynamic formulation. However, since the pioneering work of Hopf and Cole, and despite the successes in adapting statistical mechanics methods in two-dimensional turbulence [4], the precise relation between statistical physics and turbulence remains an open question.

An important breakthrough in understanding this surprising connection came in the work of Majda and Timofeyev [5] on the one-dimensional Galerkin truncated Burgers equation which, while exhibiting intrinsic chaos, has nevertheless a compact equilibrium statistical physics description. The solution to this equation was shown to thermalise, with energy equipartition, in a finite time. Subsequently, Cichowlas *et al.*, in Ref. [6] discovered through state-of-the-art direct numerical simulations (DNSs) of the finite-dimensional, truncated, in-

compressible Euler equations that the solutions in a finite time start thermalising. This process of thermalisation begins at the largest wavenumber of the system – the truncation wavenumber K_G (such that all modes with wavenumbers greater than K_G are set to zero) – and with time starts extending to smaller and smaller wavenumbers until eventually one obtains an energy spectrum $E(k) = k^2$ for all wavenumbers $1 \leq k \leq K_G$. Curiously, it was observed that at intermediate times the energy spectrum showed a transient Kolmogorov scaling $E(k) \sim k^{-5/3}$ at smaller non-thermalised wavenumbers and a scaling of $E(k) \sim k^2$ for higher wavenumbers all the way upto K_G . This seminal work thus provided the first numerical evidence of the co-existence of equilibrium micro-states along side a Kolmogorov-like turbulent cascade in inviscid, finite-dimensional equations of hydrodynamics (see also Ref. [7]).

A second, recent, breakthrough in understanding the interplay between equilibrium statistical mechanics and turbulent flows came through the development of the method of fractal Fourier decimation introduced in Ref. [8]. This novel method, which allows microsurgeries in the triadic interactions of the non-linear term, was used to show, theoretically and numerically, that there exists special dimensions where fluxless, equilibrium solutions coincide with the Kolmogorov spectrum [8] (see also Ref. [9]). Subsequently this method was used in several other studies [10–13] to understand triadic interactions *inter alia* intermittency, equilibrium solutions and turbulence.

As a result of these very recent developments [5, 6, 8, 9, 14–17] (see also Ref. [18] for a recent review), the last few years have seen a furthering in our understanding of the possible existence of equilibrium solutions in inviscid equations of hydrodynamics. Specifically, equipartition solutions to the Galerkin-truncated Gross-Pitaevskii [19], magnetohydrodynamic [20], Burgers [5, 17], and Euler equations [6, 21] have been studied extensively in recent years. Alongside the very important theoretical under-

pinnings of such studies, thermalised or partially thermalised states have been shown [22–24] to be a possible explanation of the ubiquitous bottleneck [25] in the energy spectrum of turbulent flows.

Despite the rapid advances in this field [18], an important question remains unanswered. It has been shown in earlier studies [6, 17, 18] that inviscid, truncated systems thermalise in finite times. The reason why one obtains thermalised states is of course well known [5, 17]: Galerkin-truncated (which we define precisely later) equations of ideal hydrodynamics (such as the Euler or the inviscid Burgers equation) are conserved dynamical systems with Gibbsian statistical mechanics [6, 7, 17]. A few years ago the first explanation of how such systems thermalise, through resonant wave-particle interactions mediated by structures called *tygers* was given in Ref. [17]. However a theoretical or numerical estimate of the time-scale at which thermalisation sets in has proved elusive. In this paper we address this question and show through theoretical arguments, which are substantiated by detailed numerical simulations, that the time T_c at which thermalisation sets in scales as $T_c \sim K_G^{-4/9}$, where K_G is the Galerkin truncation wavenumber (defined precisely below) in the problem.

There is one additional, applied reason for investigating the issue of the onset of thermalisation in such systems. Spectral and pseudospectral methods, especially with the advent of fast Fourier transform routines, are extremely precise techniques for numerical solutions of the nonlinear partial differential equations of hydrodynamics [26]. By definition such methods are limited by finite resolutions and hence are finite-dimensional. Therefore such numerical methods nearly always end up solving the Galerkin-truncated variant of the actual equation of hydrodynamics. In viscous calculations, such as the Navier-Stokes or the viscous Burgers equations, the difference between the true solution of the equations and its Galerkin-truncated variant is often imperceptible. However in numerical studies of the blow-up problem [27] for inviscid equations the onset of thermalised states – which are not admitted in the original infinite dimensional partial differential equation – can have grave consequences on the interpretation of numerical results.

GALERKIN TRUNCATION

Given the formidable theoretical (and even numerical) difficulties associated with the incompressible, three-dimensional Euler equations, it seems that a convenient starting point to explore the onset of thermalisation in inviscid, finite-dimensional equations of hydrodynamics is the one-dimensional Burgers equation. Given its analytical and numerical tractability, the Burgers equation has often been used with great success to establish or

disprove conjectures for problems pertaining to the Euler or Navier-Stokes equations. (We refer the reader to Refs. [28, 29] for a review of the Burgers equations and its many applications.) We should point out that even in the relatively simpler problem of the inviscid, truncated Burgers equation, the limit $K_G \rightarrow \infty$ is not a trivial one. Indeed there are examples of energy-conserving perturbations to the inviscid Burgers equation which do not necessarily converge (in a weak sense) to the inviscid limit [30].

Thus, we begin with the one-dimensional inviscid Burgers equation

$$\frac{\partial u}{\partial t} + \frac{1}{2} \frac{\partial u^2}{\partial x} = 0 \quad (1)$$

augmented by the initial conditions $u_0(x)$ which are typically a combination of trigonometric functions containing a few Fourier modes. Without any loss in generality one can choose $u_0(x) = \sin(x + \phi)$; where ϕ is some random phase. Since we work in the space of 2π periodic solutions, we can expand the solution of Eq.(1) in a Fourier series

$$u(x) = \sum_{k=0,\pm 1,\pm 2,\dots} e^{ikx} \hat{u}_k. \quad (2)$$

This allows us to naturally define the Galerkin projector P_{K_G} as a low-pass filter which sets all modes with Fourier wavenumbers $|k| > K_G$, where K_G is a positive (large) integer, to zero via

$$P_{K_G} u(x) = \sum_{|k| \leq K_G} e^{ikx} \hat{u}_k. \quad (3)$$

These definitions allow us to write the Galerkin-truncated inviscid Burgers equation as

$$\frac{\partial v}{\partial t} + P_{K_G} \frac{1}{2} \frac{\partial v^2}{\partial x} = 0; \quad (4)$$

the initial conditions $v_0 = P_{K_G} u_0$ are similarly projected onto the subspace spanned by K_G . This defines the Galerkin-truncated velocity v of the Burgers equation. For the three-dimensional Euler equations, the same definition follows *mutatis mutandis*.

The inviscid Burgers equation (1) conserves all moments of the velocity field; by contrast the Galerkin-truncated version of it (4) retains only the first three moments of v , and in particular the energy. Numerically, however, the dynamics of the Galerkin-truncated Burgers captures rather well the blowing up (with smooth initial conditions) of the gradient of the solution to the inviscid Burgers partial differential equation in a finite time t_* . Indeed the cubic-root singularity (preshock), at $t_* = \frac{1}{\max[\partial_x u]} \approx \frac{1}{\max[\partial_x v]}$, in u (1) is also seen in the solution v of the Galerkin-truncated equation [17, 28, 29, 31]. Theoretically, the solution to (1) for times greater than

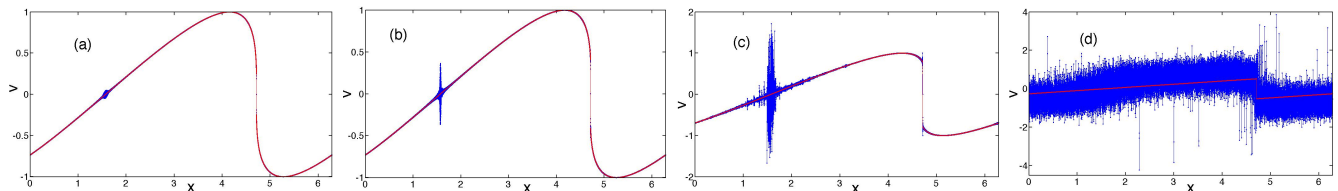


FIG. 1. Solution of the Galerkin-truncated Burgers equation (4) v (in blue) and the un-truncated Burgers equation (1) (entropy solution) u (in red) at different times for the initial condition $v_0 = u_0 = \sin(x + \phi)$ at different times $t \gtrsim t_*$. At early times (a) $t = 1.01$ the discrepancy between the two is small and localised around $x = x_{\text{tyger}}$ where the velocity is identical to that of the shock. This discrepancy, the tyger, grows (still remaining localised in space) in time as shown in (b) with $t = 1.03$. At a later time (c) $t = 1.15$, the symmetric, localised structure becomes asymmetric and starts spreading away from x_{tyger} . Even at this time the truncated solution is able to duplicate the entropy solution at regions far away from x_{tyger} and in particular is able to capture the location and amplitude of the shock. At much later times, (d) $t = 5.0$, the solution v thermalises and becomes Gaussian, does not display the shock, and shows no similarity with the entropy solution u . This set of representative plots showing the birth and growth of tygers followed by the onset and eventual thermalisation of the solution were obtained from simulations with $K_G = 5000$ and $N = 2^{16}$.

t_* is obtained by adding a tiny viscous dissipation term $\nu \frac{\partial^2 u}{\partial x^2}$, with $\nu \rightarrow 0$ (the inviscid limit), which yield, depending on the initial conditions, finitely many shocks for times $t > t_*$ [1]. This generalised solution, which converges weakly to the inviscid Burgers equation (1), is characterised by the dissipative anomaly: energy dissipation ϵ remains finite (with an associated non-conservation of the total energy) as $\nu \rightarrow 0$. This is very different to the dynamics of the Galerkin-truncated equation (4) whose solution v stays smooth, conserves energy for all times $t > t_*$ and later thermalises.

SIMULATION DETAILS

We perform extensive and state-of-the-art simulations to obtain solutions for u (1) and v (4) for all times.

The true or entropy solution to the inviscid Burgers equation (1) is obtained by the method of Fast Legendre Transform, which takes the limit $\nu \rightarrow 0$, developed by Noullez and Vergassola [32] (see also Refs. [33, 34]). This method takes advantage of the fact [28, 29] that the velocity potential ψ defined via $u = -\frac{\partial \psi}{\partial x}$ is constrained by the maximum principle such that

$$\psi(x, s) = \max_y \left[\psi(y, t) - \frac{(x - y)^2}{2(s - t)} \right]; \quad (5)$$

where $s > t$. We typically use the number of collocation points $N = 2^{14}$ or 2^{16} and choose a time step δt large enough for a Lagrangian particle[?] to move by a distance equal to or larger than the grid spacing δx , and smaller than all other time scales associated with the dynamics.

We, of course, use a different strategy to solve the Galerkin-truncated equation (4). We use a pseudo-spectral method [26] coupled to a fourth-order Runge-Kutta time marching with the total collocation points $N = 2^{14}$ or 2^{16} as before. We use different values of

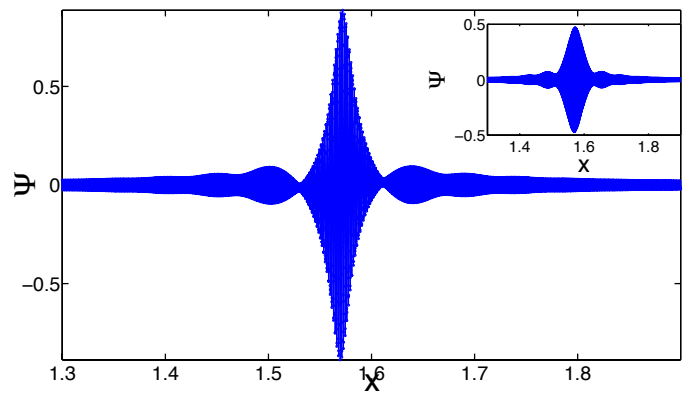


FIG. 2. A representative zoomed-in plot of the discrepancy $\Psi = v - u$, around x_{tyger} for $K_G = 4000$ just when the bulge becomes asymmetric $t = T_c$ and (inset) when it is still symmetric $t < T_c$. The tyger, apart from being localised, is monochromatic with a single wavenumber K_G before T_c (inset) [17]; for $t \geq T_c$, other harmonics smaller than K_G are generated as well.

K_G , ranging from 700 to 20,000. Our time step δt varied from 10^{-4} for $K_G \leq 5,000$ to 10^{-5} for $K_G > 5,000$. Full dealiasing was ensured in this problem via K_G .

RESULTS

Tygers and Thermalisation

We begin by performing direct numerical simulations of equations (1) and (4), without any loss of generality [17, 18], with initial conditions $u_0(x) = v_0(x) = \sin(x + \phi)$, where $\phi = 0.7$ is a phase which shifts the location of the cubic singularity away from $x = \pi$. For such an initial condition, it is easy to show that $t_* = 1.0$ [28, 29]. The time evolution of the solution to the untruncated Burgers equation $u(x)$ and the trun-

cated Burgers equation $v(x)$ are shown in Fig. 1. For times $t \lesssim t_\star = 1.0$, $v = u \forall x$ as shown before [?]. At $t = t_\star$ (in this case $t_\star = 1.0$) and thereafter the discrepancy between the entropic solution $u(x)$ (in red) and $v(x)$ (in blue) is large as seen in Fig. 1. At early times, $t \gtrsim t_\star$, this discrepancy is localised (Figs. 1a and 1b); at later times (Fig. 1c) the solution to the Galerkin truncated equation starts deviating strongly from the entropy solution till at very large times it thermalises and shows a white-noise behaviour markedly different from the sawtooth entropic solution (Fig. 1d).

A useful framework to study the departure from the entropy solution to the thermalised solution is via the discrepancy $\Psi = v - u$. For $t \lesssim t_\star$, $\Psi = 0$. However, as shown in Ref. [17], at $t = t_\star$, at points which have the same velocity as the shock(s), $\Psi \neq 0$ and a symmetric, localised, monochromatic bulge, called *tyger* by Ray, *et al.* [17], forms as shown in Fig. 2 (inset). As time evolves, this bulge grows in amplitude α and width β , becomes asymmetric (Fig. 2, at $t = 1.07$), collapses, delocalises, and eventually invades the whole 2π -domain (Figs. 1c and 1d).

We now know that finite-dimensional equations of hydrodynamics thermalise through wave-particle resonances. Such resonances at early times manifest themselves as localised structures at the instant $t_G \lesssim t_\star$, when complex singularities are within one Galerkin wavelength $\lambda_G = \frac{2\pi}{K_G}$ of the real domain. This was shown to be true for both the compressible Burgers equation as well as the incompressible Euler equations [17, 18]. Indeed the scaling properties of the early tygers at $t = t_\star$ were derived in Ref. [17] and in particular the amplitudes and widths were shown to scale as $\alpha \sim K_G^{-2/3}$ and $\beta \sim K_G^{-1/3}$, respectively. Finally it was shown through detailed numerical simulations that in a short time these monochromatic, with wavelength λ_G , localised, symmetric tygers become skewed, *collapse*, and spread throughout $0 \leq x \leq 2\pi$, generate other harmonics, and eventually result in a thermalised solution with energy equipartition $E(k) \sim k^0$. However the critical question of the time T_c when thermalisation is triggered has been left unanswered in previous studies. In this work we obtain a precise estimate of T_c as a function of K_G and substantiate our theoretical prediction through detailed numerical simulations.

Onset time

Before we present our theoretical prediction for T_c , it is important at this stage to provide a more precise definition of this time.

Detailed numerical simulation show (Figs. 1 and 2 as well as in Ref. [17]) that in the early stages $t \gtrsim t_\star$ the discrepancy Ψ is small and localised at $x = x_{\text{tyger}}$, where x_{tyger} are points co-moving with the shock. With time this bulge becomes bigger (still symmetric and

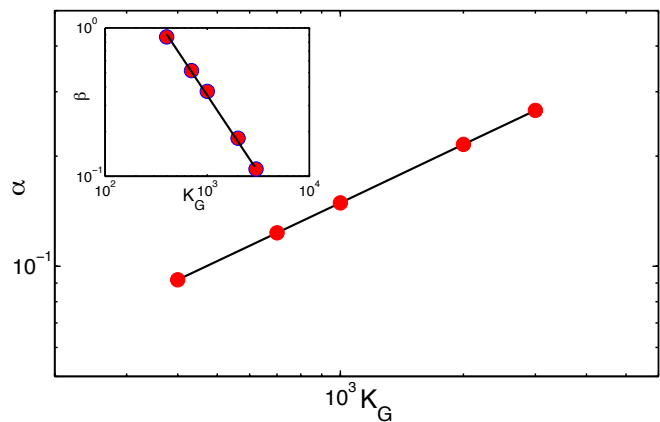


FIG. 3. (Log-log plots of the tyger amplitudes α and widths β (inset), shown by large red dots, versus K_G at a fixed time $t = 1.05$ from our simulations. The thick black line, both in the inset and the main figure, correspond to the theoretical prediction of $\beta \sim K_G^{-1}$ and $\alpha \sim K_G^{1/2}$, respectively. We find remarkable agreement between our analytical prediction and numerical data. We note that for reasons outlined in the text, we show data for values of K_G for which $T_c > 1.05$.

localised), narrower (see Fig. 2), and the associated Reynolds stresses start increasing. At a critical time, the Reynolds stress becomes large enough to make the bulge asymmetric. This leads to a collapse of the bulge, accompanied by a spatial spreading of the oscillations as well as the generation of different harmonics, and the triggering of thermalisation of the system. We define this critical time T_c as the time for onset of thermalisation. We note that numerically T_c is well-defined and easy to measure given that the asymmetry in the bulge Ψ can be determined clearly from the difference in the position of the positive and negative peaks: This difference is zero for $t_\star \leq t \leq T_c$ and becomes non-zero for $t > T_c$.

Before we proceed further, it is important at this stage to define the nomenclature which we will use in obtaining our estimate for the time of the onset of thermalisation. As defined before, $t_\star = \frac{1}{\max[\partial_x u]} \approx \frac{1}{\max[\partial_x v]}$ is the time when the complex singularity reaches the real domain. It was shown that [17] tygers are born at a slightly earlier time T_b such that $\tau_b \equiv t_\star - T_b = \mathcal{O}(K_G^{-2/3})$. We define a new time scale $\tau_c \equiv T_c - T_b$ which gives the estimate of the time scale for the onset of thermalisation[?] and we obtain theoretical results for the shifted time $\tau \equiv t - T_b$. It should be noted that this is a natural choice for time since for $t < T_b$ tygers do not exist. We will see below that τ_c indeed shows a power-law behaviour in K_G with a scaling form $\tau_c \sim K_G^\xi$; in what follows we derive an explicit form for this new scaling exponent ξ and verify our theoretical predictions with data from detailed numerical simulations.

We now turn our attention to the amplitude α and

	$\alpha \sim \tau^{\gamma_\alpha} K_G^{\delta_\alpha}$		$\beta \sim \tau^{\gamma_\beta} K_G^{\delta_\beta}$		$\tau_c \sim K_G^\xi$
	γ_α	δ_α	γ_β	δ_β	ξ
Theory	7/4	1/2	-1	-1	$\xi = \frac{\delta_\beta - 2\delta_\alpha}{2\gamma_\alpha - \gamma_\beta} = -4/9$
Simulations	1.74 ± 0.04	0.50 ± 0.01	-0.97 ± 0.08	-1.01 ± 0.02	-0.46 ± 0.07

TABLE I. A summary of the new scaling exponents that we derive in this work. We see an excellent agreement, within error-bars, between our theoretical prediction and the exponents obtained, independently, from direct numerical simulations.

width β of the tyger. Let the widths and amplitudes assume the scaling form $\beta \sim \tau^{\gamma_\beta} K_G^{\delta_\beta}$ and $\alpha \sim \tau^{\gamma_\alpha} K_G^{\delta_\alpha}$, respectively. It is important to note that the scaling ansatz introduced here for the widths and amplitudes of the bulge (tyger) at any time $\tau \equiv t - T_b$ is consistent with the result introduced in the previous section (and proved in [17]), namely the width and amplitude of the tyger at t_* . This is because at $t = t_*$, $\tau = \tau_b \sim K_G^{-2/3}$ (see [17]) and hence the scaling relation of the previous section follows from this ansatz. This is an important check of self-consistency of the theory. The asymmetry in the bulge occurs when the gradient of the Reynolds stresses become order one at time τ_c . The Reynolds stress is defined as $\overline{\Psi^2}$, where the overline indicates the typical, *mesoscopic* average (spatial) (α) over lengthscale larger than the Galerkin wavelength but smaller than other macroscopic scales in the problem; thence, dimensionally, the gradient of the Reynolds stress, namely $\frac{\alpha^2}{\beta}$, follows, since the relevant length scale over which this gradient should be taken $\sim \beta$. By using the assumed scaling form for α and β one obtains the scaling form for the time of the onset of thermalisation as

$$\tau_c \sim K_G^\xi \sim K_G^{\frac{\delta_\beta - 2\delta_\alpha}{2\gamma_\alpha - \gamma_\beta}}. \quad (6)$$

We thus obtain the first theoretical estimate for the onset time of thermalisation in a truncated equation of idealised hydrodynamics and obtain a new scaling exponent for the same, namely,

$$\xi = \frac{\delta_\beta - 2\delta_\alpha}{2\gamma_\alpha - \gamma_\beta}. \quad (7)$$

It now behoves us to determine, self-consistently, the exponents γ_α , γ_β , δ_α , and δ_β and verify our predictions from detailed numerical simulations.

As we know that the Galerkin-truncated Burgers equation conserves energy for all time while displaying spatio-temporal chaotic behaviour at time $t \gg t_*$. This is unlike the case of the entropy or untruncated solution u of (1) which dissipate energy ϵ_{shock} through the shock for time $t \geq t_*$. Therefore for the truncated equation to conserve energy, ϵ_{shock} gets transferred to the tygers via a resonant-wave-particle mechanism. Given that the estimate of energy contained in the tyger is $\alpha^2\beta$, this implies that for different values of K_G , the energy content of the tyger must be the same. This immediately suggests that

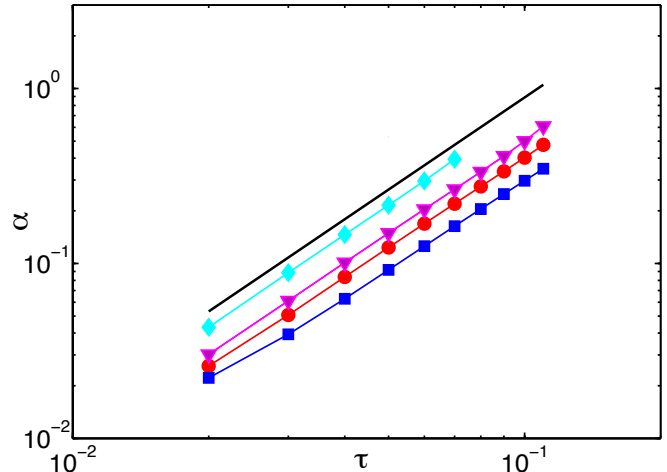


FIG. 4. Log-log plots of the tyger amplitudes α , for various values of the truncation wavenumber K_G , as a function of the shifted time τ . The different set of symbols correspond to different values of K_G , namely, blue filled squares for $K_G = 400$; big red dots for $K_G = 700$; filled pink triangles for $K_G = 1000$; and filled cyan diamond for $K_G = 2000$. For each value of K_G , our theoretical prediction $\alpha \sim \tau^{7/4}$, shown via thick black lines, seems to be in excellent agreement with the numerical data.

for any finite τ , the integral $\int_0^\tau \alpha^2 \beta dt$ is independent of K_G . By using this argument we obtain the relation

$$2\delta_\alpha + \delta_\beta = 0. \quad (8)$$

Spatially the tygers are confined, due to resonance, to a region of width w . For the tyger to grow, coherently, in a time interval τ , phase mixing constrains this region to be of an extent such that the velocity difference across w is of the order of λ_G/τ . Since $\lambda_G = 2\pi/K_G$ and the velocity difference across w is proportional to w , this implies that

$$\beta \sim \frac{1}{\tau K_G} \quad (9)$$

yielding the exponents $\gamma_\beta = \delta_\beta = -1$. Furthermore, from (8), we obtain $\delta_\alpha = 1/2$.

In Fig. 3 we show plots of α and β (inset) at a given time $t = 1.05$ as a function of K_G . The thick black line connecting our data from numerical simulations (shown as large red dots) correspond to the theoretical prediction

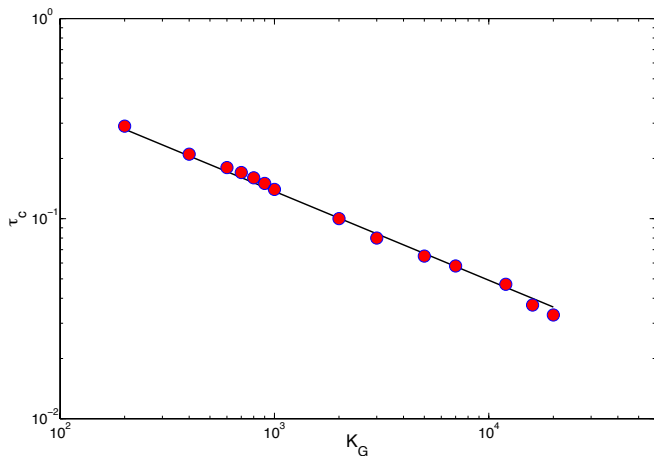


FIG. 5. Log-log plot of the onset time τ_c for thermalisation versus K_G . The data from our simulations is shown by big red dots; the thick black line connecting the data points is the theoretical prediction $\tau_c \sim K_G^{-4/9}$. Note the excellent agreement between our data and the theoretical prediction for smaller values of K_G as compared to the larger values of K_G . Possible reasons for this discrepancy is discussed in the text.

of $\delta_\alpha \sim K_G^{1/2}$ and $\delta_\beta \sim 1/K_G$. The figure shows not only a clear scaling, for both, but also an excellent agreement of our numerical data with our theoretical predictions as well as validating our assumptions in arriving at our analytical results. We note that the range of K_G shown in this figure does not extend all the way to our full range (e.g., see Fig. 5). This is because at the time $t = 1.05$, for which the data is shown, solutions to the truncated equation with K_G greater than 3000 have already thermalised (see Fig. 5); hence the tygers have already collapsed for such wavenumbers at $t = 1.05$ and thus the measurement of their amplitudes and widths do not make sense. Our choice of $t = 1.05$ is motivated by having a time reasonably larger than t_\star for which we still have a large range in K_G to clearly illustrate the theoretically predicted scaling behaviour.

Finally let us determine γ_α . Let us consider $t = t_\star$, which, as we have noted before and proved in Ref. [17], implies $\tau \sim K_G^{-2/3}$. At time t_\star , the untruncated equation shows a cubic root singularity. This implies, that because of Galerkin truncation the energy lost in the shock – and hence gained as $\alpha^2\beta$ in the tyger – is estimated as $\int_0^{\lambda_G} x^{2/3} dx \sim K_G^{-5/3}$. Setting $\tau = K_G^{-2/3}$, and using our previously obtained estimate $\gamma_\beta = \delta_\beta = -1$ and $\delta_\alpha = 1/2$, this suggests that

$$K_G^{\frac{-4\gamma_\alpha+2}{3}} \sim K_G^{-5/3}. \quad (10)$$

Hence we obtain $\gamma_\alpha = 7/4$.

From our simulations we calculate α for different values of K_G and show plots α vs τ for representative values

of K_G in Fig. 4. The thick black line, which is $\propto \tau^{7/4}$ is our theoretical prediction that for a given value of K_G , the amplitude of the tyger (upto the time of collapse) scales as $\alpha \sim \tau^{7/4}$. As in Fig. 3, we find excellent agreement between data obtained from our simulations with the theoretical prediction.

Having obtained theoretically, and validated through simulations (Figs. 3 and 4), the values of the scaling exponents of the amplitude and width of the tygers before they collapse, let us once again return to the issue of the scaling of the onset time of thermalisation τ_c . We had obtained before the scaling form of τ_c in Eq. 6. We now use the values of the various exponents obtained thence to show, from Eq. 7, that $\xi = -4/9$, implying that thermalisation is triggered at a time

$$\tau_c \sim K_G^{-4/9}. \quad (11)$$

A summary of all these exponents is given in Table 1.

We now turn to our numerical simulations and obtain, for different values of K_G , the time of collapse τ_c . In our numerical simulations we actually measure τ_c by using t_\star (instead of T_b) as the reference time, i.e., $\tau_c \equiv T_c - t_\star$. The reason for this is because for the simulations we wanted a unique reference time t_\star which is independent of K_G (unlike T_b). This also reduces significantly any measurement error in estimating T_b . Such a definition of τ_c , for our numerical simulations, is justified because for the values of K_G used in our simulations, T_b and t_\star are extremely close to each other [17] and there is an order of magnitude separation between the time scales τ_b and τ_c .

In Fig. 5, we show (red dots) the data obtained from our simulations. The thick black line corresponds to the theoretical prediction (11). We find excellent agreement between our analytical prediction and the data obtained from simulations. Despite this confirmation of our theoretical predictions, it is important to note that at extremely large values of K_G we see a noticeable discrepancy between the theoretical result and our data. The reasons for this are two-fold: Firstly, as K_G becomes larger and larger, τ_c become smaller and smaller. Hence a very accurate measurement of τ_c , numerically, becomes harder because the relative error between the temporal resolution of our simulations and τ_c become larger. A second reason for this is that numerically, for reasons mentioned before, we measure τ_c relative to t_\star and not T_b . Hence for large K_G when τ_c becomes smaller, our neglecting of τ_b (although there is an order of magnitude scale separation between τ_c and τ_b) probably starts yielding a correction which is less negligible.

CONCLUSIONS

In this paper we provide the first prediction, analytically and validated by numerically simulations, of

the time when thermalisation is triggered in finite-dimensional inviscid equations of hydrodynamics and hence solves a very important problem in the interface of turbulence and statistical mechanics. We show that, through the Galerkin-truncated Burgers model, thermalisation is triggered on a time scale which decays as a power-law in K_G with an exponent which has been derived analytically by us and verified through numerical simulations.

Our results throw up important implications beyond the obvious realms of non-equilibrium statistical physics. This has to do with using numerical simulations for tracing complex singularities, in ideal equations of hydrodynamics, by using the method of the analyticity strip [35]. In recent years (we refer the reader to Ref. [36] for the most recent results and to Ref. [27] for a recent review of results on finite-time blow-ups via numerical simulations), with the advance of computing power, the search for evidence for or against finite-time blow-up of the three-dimensional Euler equations through numerical simulations have gained ground. As shown by Bustamante and Brachet [36], the temporal measurement of the distance, to the real domain, of the nearest singularity, is limited not only by computing power but also by the onset of thermalisation. Hence an estimate of the time when thermalisation sets in will be have an important bearing on interpreting the accuracy of measurements of complex singularities in time from spectral, and hence Galerkin-truncated, simulations of the Euler equations. We note in passing that the limitation in extrapolating in time the temporal evolution of the width of the analyticity strip has been noted, amongst others, in Ref. [36].

There are of course several important questions which still remain unanswered. Foremost amongst them is the need to see, numerically, if a similar scaling argument holds for the incompressible three-dimensional Euler equation. This is a massively challenging task even with the modern day computers. Secondly the onset of thermalisation is necessarily accompanied by the generation of Fourier harmonics other than K_G which eventually lead to a white noise velocity field with a flat spectrum. The precise mechanism of this is yet to be understood in an analytical way. Furthermore, it has been observed (Fig. 2 as well as in Ref. [17]) that just prior to and after τ_c , secondary bulges, reminiscent of the beating effect in acoustics, develop on either side of the tyger. A systematic theory which explains the full transition to thermalised states should capture this effect. These questions, and many more, are left for future work.

We thank Aritra Kundu for many useful discussions. Both authors acknowledge financial support from the AIRBUS Group Corporate Foundation Chair in Mathematics of Complex Systems established in ICTS-TIFR. SSR also acknowledges the support from DST (India) project ECR/2015/000361 and the Indo-French Center

for Applied Mathematics (IFCAM). The direct numerical simulations were done on *Mowgli* at the ICTS-TIFR, Bangalore, India.

* Presently at the Department of Mathematics, Institute of Chemical Technology, Mumbai, India; vdivya8@yahoo.co.in

† samriddhisankarray@gmail.com

- [1] E. Hopf, *Comm. Pure Appl. Math.* **3**, 201 (1950).
- [2] T. D. Lee, *Q. J. Appl. Math.* **10** (1952).
- [3] A.N. Kolmogorov, *Dokl. Akad. Nauk SSSR* **30**, 301 (1941); A.N. Kolmogorov, *Dokl. Akad. Nauk SSSR* **31**, 538 (1941).
- [4] R. Kraichnan, *Phys. Fluids* **10**, 1417 (1967).
- [5] A. J. Majda and I. Timofeyev, *Proc. Natl. Acad. Sci.* **97** 12413 (2000).
- [6] C. Cichowlas, P. Bonaïti, F. Debbash, and M. Brachet, *Phys. Rev. Lett.* **95**, 264502 (2005).
- [7] R. H. Kraichnan and S. Chen, *Physica D* **37**, 160 (1989).
- [8] U. Frisch, A. Pomyalov, I. Procaccia, and S. S. Ray, *Phys. Rev. Lett.* **108**, 074501 (2012).
- [9] V. L'vov, A. Pomyalov and I. Procaccia, *Phys. Rev. Lett.* **89**, 064501 (2002).
- [10] M. Buzdicotti, L. Biferale, U. Frisch, and S. S. Ray, *Phys. Rev. E* **93**, 033109 (2016).
- [11] A. S. Lanotte, R. Benzi, S. K. Malapaka, F. Toschi, and L. Biferale, *Phys. Rev. Lett.* **115**, 264502 (2015).
- [12] A. S. Lanotte, S. K. Malapaka, L. Biferale, *Eur. Phys. J. E* **39**, 49 (2016).
- [13] M. Buzdicotti, A. Bhatnagar, L. Biferale, A. S. Lanotte, S. S. Ray, *New J. of Phys.* **18**, 113047 (2016).
- [14] V. S. L'vov, S. V. Nazarenko, and O. Rudenko, *Phys. Rev. B*, **76**, 024520 (2007).
- [15] C. Connaughton, *Physica D*, **238**, 2282 (2009).
- [16] P. Feng, J. Zhang, S. Cao, S.V. Prants, Y. Liu, *Commun. Nonlinear Sci. Numer. Simulat.*, **45**, 104 (2017)
- [17] S. S. Ray, U. Frisch, S. Nazarenko, and T. Matsumoto, *Phys. Rev. E* **84**, 16301 (2011).
- [18] S. S. Ray, in *Persp. in Nonlinear Dynamics*, *Pramana - J. of Phys.*, **84**, 395, (2015).
- [19] G. Krstulovic and M. Brachet, *Phys. Rev. Lett.*, **106**, 115303 (2011); G. Krstulovic and M. Brachet, *Phys. Rev. E*, **83**, 066311 (2011); V Shukla, M Brachet, R Pandit, *New Journal of Physics*, **15**, 113025 (2013).
- [20] G. Krstulovic, M. E. Brachet, and A. Pouquet, *Phys. Rev. E*, **84**, 016410 (2011).
- [21] G. Krstulovic, P. D. Mininni, M. E. Brachet, and A. Pouquet, *Phys. Rev. E*, **79**, 056304 (2009).
- [22] U. Frisch, S. Kurien, R. Pandit, W. Pauls, S. S. Ray, A. Wirth, and J-Z Zhu, *Phys. Rev. Lett.* **101**, 144501 (2008).
- [23] U. Frisch, S. S. Ray, G. Sahoo, D. Banerjee, and R. Pandit, *Phys. Rev. Lett.*, **110**, 64501 (2013).
- [24] D. Banerjee and S. S. Ray, *Phys. Rev. E* **90**, 041001(R) (2014).
- [25] W. Dobler, N.E.L. Haugen, T.A. Yousef and A. Brandenburg, *Phys. Rev. E*, **68**, 026304 (2003); Z.-S. She, G. Doolen, R.H. Kraichnan, and S.A. Orszag, *Phys. Rev. Lett.*, **70**, 3251 (1993); P.K. Yeung and Y. Zhou, *Phys. Rev. E*, **56**, 1746 (1997); T. Gotoh, D. Fukayama, and T.

- Nakano, *Phys. Fluids*, **14**, 1065 (2002); M.K. Verma and D.A. Donzis, *J. Phys. A: Math. Theor.*, **40**, 4401 (2007); P.D. Mininni, A. Alexakis, and A. Pouquet, *Phys. Rev. E*, **77**, 036306 (2008). Y. Kaneda, *et al.*, *Phys. Fluids*, **15**, L21 (2003); T. Isihara, T. Gotoh, and Y. Kaneda *Annu. Rev. Fluid Mech.*, **41**, 165 (2009); S. Kurien, M.A. Taylor, and T. Matsumoto, *Phys. Rev. E*, **69**, 066313 (2004); D.A. Donzis and K.R. Sreenivasan *J. Fluid Mech.*, **657**, 171 (2010); H.K. Pak, W.I. Goldburg, A. Sirivat, *Fluid Dynamics Research*, **8**, 19 (1991); Z.-S. She and E. Jackson, *Phys. Fluids A*, **5**, 1526 (1993); S.G. Saddoughi and S.V. Veeravalli, *J. Fluid Mech.*, **268**, 333 (1994); G. Falkovich, *Phys. Fluids*, **6**, 1411 (1994); L. Sirovich, L. Smith, and V. Yakhot, *Phys. Rev. Lett.*, **72**, 344, (1994).
- [26] D. Gottlieb and S. A. Orszag, *Numerical analysis of spectral methods: theory and applications*, CBMS-NSF Regional Conference Series in Applied Mathematics **26**, SIAM (1977).
- [27] U. Frisch, T. Matsumoto, and J. Bec, *J. Stat. Phys.* **113**, 761 (2003); J. D. Gibbon, *Physica D* **237**, 1894 (2008).
- [28] U. Frisch and J. Bec, *Les Houches 2000: New Trends in Turbulence*, Eds. : M. Lesieur, A. Yaglom and F. David, pp. 341-383, Springer EDP-Sciences, (2001).
- [29] J. Bec and K. Khanin, *Phys. Rep.* **447**, 1-66, (2007).
- [30] P. D. Lax and C. D. Levermore, *Proc. Natl. Acad. Sci. U.S.A.* **76**, 3602 (1979); J. Goodman and P. D. Lax, *Commun. Pure Appl. Math.* **41**, 591 (1988); T. Y. Hou and P. D. Lax, *Commun. Pure Appl. Math.* **44**, 1 (1991).
- [31] J.D. Fournier and U. Frisch, *J. Méc. Théor. Appl. (Paris)* **2**, 699 (1983).
- [32] A. Noullez and M. Vergassola, *J. Sci. Comp.* **9**, 259 (1994).
- [33] J. Bec, U. Frisch, and K. Khanin, *J. Fluid Mech.* **416**, 239 (2000).
- [34] D. Mitra, J. Bec, R. Pandit, and U. Frisch, *Phys. Rev. Lett.* **94**, 194501, (2005).
- [35] C. Sulem, P.-L. Sulem, H. Frisch, *J. Comput. Phys.* **50**, 138 (1983).
- [36] M. D. Bustamante and M. Brachet, *Phys. Rev. E* **86**, 066302 (2012).